

Multicolor Femtosecond Laser with μJ Level by Cascaded Four-Wave Mixing

Takayoshi KOBAYASHI^{1,2,3,4*} and Jun LIU^{1,2}

¹Department of Applied Physics and Chemistry and Institute for Laser Science, University of Electro-Communications, 1-5-1 Chofugaoka, Chofu, Tokyo 182-8585, Japan

²International Cooperative Research Project (ICORP), Japan Science and Technology Agency, 4-1-8 Honcho, Kawaguchi, Saitama 332-0012, Japan

³Department of Electrophysics, National Chiao Tung University, 1001 Ta Hsueh Rd., Hsinchu 300, Taiwan

⁴Institute of Laser Engineering, Osaka University, 2-6 Yamada-oka, Suita, Osaka 565-0871, Japan

(Received August 26, 2009; Accepted December 27, 2009)

Tunable multicolor femtosecond pulses were simultaneously obtained by a cascaded four-wave mixing process in a fused-silica glass plate. Frequency up-shift and down-shift pulses with energies of about $1\ \mu\text{J}$ and durations of 45 fs sidebands were obtained. When one of the two input beams was negatively chirped and the other was positively chirped, self-compressed multicolor 20 fs pulses, which were nearly transform limited, were obtained.

© 2010 The Japan Society of Applied Physics

Keywords: four-wave mixing, multicolor, femtosecond, negative chirp

1. Introduction

Over the past decade, tunable femtosecond laser systems in the visible light region have been developed using a noncollinear optical parametric amplifier (NOPA) based on three-wave mixing in a nonlinear crystal.¹⁾ Recently, interest in four-wave mixing (FWM) has been growing as an alternative.^{2–5)} Multicolor sidebands were generated in BK7 glass,²⁾ in fused silica glass,^{3–5)} and in a sapphire plate⁶⁾ using two crossed femtosecond laser beams. Cascaded FWM (CFWM) has several advantages in obtaining tunable femtosecond pulses over the NOPA method. First, several frequency up-shifted and down-shifted multicolor femtosecond pulses can be generated at the same time and can be spatially well separated. Therefore, they are self-synchronized and convenient for multicolor pump–probe experiments, for example, those involving femtosecond coherent anti-Stokes Raman scattering (CARS) spectroscopy⁷⁾ and two-dimensional spectroscopy.⁸⁾ Second, CFWM can occur in nearly all transparent media. Hence, it is much less expensive to use glass in comparison with a nonlinear crystal. Third, CFWM can be easily extended to UV and IR regions by using a suitable medium and input parameters. Fourth, there is no need to setup a complex dispersive compensation system in the CFWM process. Fifth, in principle CFWM can be scaled into a much higher energy output because there is no limit for obtaining a large glass plate.

In this study, microjoule tunable femtosecond pulses at different wavelengths were obtained and investigated in detail in a fused silica glass plate. Self-compressed multicolor 20 fs pulses, which were nearly transform limited, were obtained.

2. Theoretical Analysis

CFWM can be described using a phase-matching con-

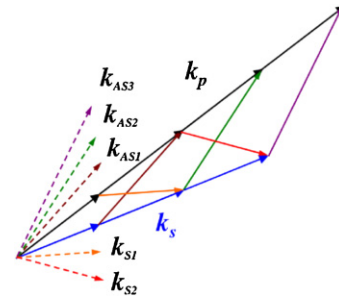


Fig. 1. (Color online) Phase-matching geometry for cascaded four-wave mixing process.

dition, as shown in Fig. 1. k_1 and k_2 are the two input beams with respective frequencies of ω_1 , ω_2 ($\omega_1 > \omega_2$). The m th-order anti-Stokes sideband will have the following phase-matching conditions: $k_{ASm} = k_{AS(m-1)} + \tilde{k}_1 - k_2 = (m+1)\tilde{k}_1 - mk_2$ and $\omega_{ASm} = (m+1)\omega_1 - m\omega_2$. ASm refers to the generated m -order anti-Stokes sideband.

3. Experimental Setup

In the experiment, femtosecond laser pulses with 40 fs/1 kHz/2.5 mJ/800 nm from a regenerative amplifier system (Micra+Legend-USP) were divided into three parts. One beam (beam 1) was spectrally broadened and then compressed in a hollow fiber system, and transmitted through a band-pass filter with a 700 nm central wavelength and a 40 nm bandwidth. Another beam (beam 2) passed through a delay stage. Beam 1 and beam 2 were focused into a 1-mm-thick fused silica glass plate with a small crossing angle. The third beam (beam 3) was used to generate cross-correlation signals with the two input beams and the sidebands in a $10\ \mu\text{m}$ BBO crystal so as to measure the pulse durations of the beams.

*E-mail address: kobayashi@ils.uec.ac.jp

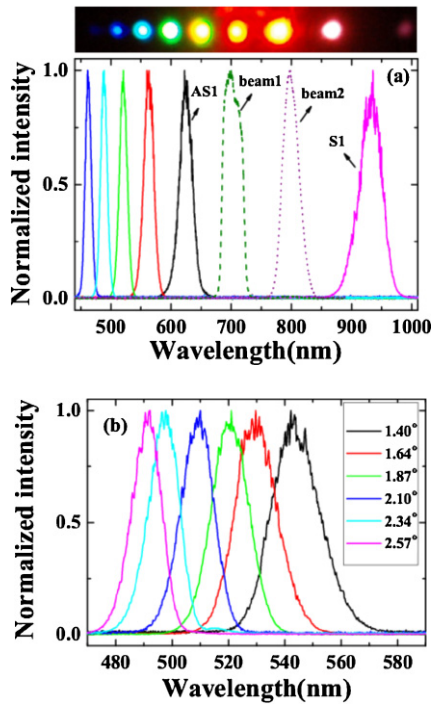


Fig. 2. (Color online) (a) Spectra of the sidebands from S1 to AS5 and of the two input beams at crossing angle of 1.87° . (b) Spectra of AS3 at crossing angles of 1.40° , 1.64° , 1.87° , 2.10° , 2.34° , and 2.57° . The photograph on top of Fig. 1(a) shows the sidebands on a sheet of white paper placed 30 cm after the glass plate at the crossing angle of 1.87° . The first, second, and third spots from the right edge indicate S1, beam 2, and beam 1, respectively.

The pulse durations of beam 1 and beam 2 were 40 ± 3 and 55 ± 3 fs, respectively. The beam radii of beam 2 were 500 and $300 \mu\text{m}$ in the horizontal and vertical directions, respectively. For beam 1, the beam radii were 440 and $285 \mu\text{m}$ in the horizontal and vertical directions, respectively. Owing to their elliptical shapes, the two input beams could overlap well in the medium even if they were crossed.

4. Results and Discussion

Cascaded multicolour FWM signals appeared individually in space on both sides of the two input beams as they were synchronously focused on the fused silica glass in both time and space. The two input beams and the generated sidebands were horizontally polarized. The photograph on top of Fig. 2(a) shows FWM sideband signals on a white sheet of paper placed about 30 cm after the glass plate. The input powers of beam 1 and beam 2 were 9 and 20 mW, respectively. Figure 2(a) shows the spectra of the sidebands from the first-order Stokes (S1) to the fifth-order anti-Stokes (AS5) cascaded FWM signals along with the spectra of two input beams at a crossing angle of 1.87° . The spectra extended from 450 to 1000 nm. The sidebands had a Gaussian profile and each anti-Stokes spectrum supported a transform-limited pulse duration of about 25 fs. Moreover, as indicated in Fig. 2(b), the peak wavelength of AS3 was tuned from 490 to 545 nm by changing the crossing angle from 1.40° to 2.57° with an angle precision of $\pm 0.02^\circ$.

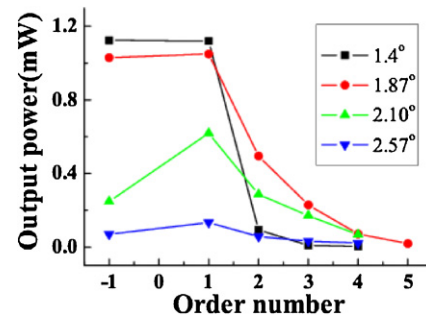


Fig. 3. (Color online) Dependence of the output power on the order number at crossing angles of 1.40° , 1.87° , 2.10° , and 2.57° between two input beams. Order number -1 refers to S1, 1 refers to AS1, and so on.

The output pulse energies of AS1 and S1 were 1.03 and $1.05 \mu\text{J}$, respectively, when the crossing angle was 1.87° , and the input average powers of beam 1 and beam 2 were 9 and 20 mW, respectively. Figure 3 shows the dependence of output power on order number at the crossing angle of 1.40° , 1.87° , 2.10° , and 2.57° between the two input beams. The output powers of S1 and AS1 decreased rapidly as the crossing angle increased from 1.40° to 2.57° . For a smaller crossing angle, for example, 1.40° , the output power of the sidebands decreased rapidly with increasing order number. However, for a larger crossing angle, for example, 2.57° , the output power of the sidebands decreased gradually with increasing order number. The energy conversion efficiency from the two input beams to the sidebands was about 10% when the crossing angle was 1.87° .

The pulse durations of S1, AS1, and AS2 were measured by using the cross-correlation frequency resolved optical gating technique (XFROG). At the crossing angle of 1.87° , the recovered intensity profiles and phases of AS1 and AS2 are shown in Fig. 4(a). The pulse durations of AS1 and AS2 were thereby found to be 45 ± 3 and 44 ± 3 fs, respectively. Figure 4(b) shows the recovered pulse profile and phase of S1. The pulse duration was 46 ± 3 fs. The retrieved phase showed that there was some chirp in the pulses due to the small positive chirp of the input pulses and the dispersion of the glass.

When the pulse duration of beam 2 was 75 fs with a positive chirp and that of beam 1 was 50 fs with a negative chirp, a 20 fs self-compressed pulse was obtained.⁵⁾ Figures 5(a) and 5(b) show the temporal profiles and phases of AS1, and the retrieved spectra and spectral phases of AS1, respectively. The pulse duration of AS1 was 20 fs, which was very close to the transform-limited pulse duration of AS1 (18 fs) and even shorter than the transform-limited pulse durations of the two input beams, which were 32 and 33 fs for beams 1 and 2, respectively.

The electric field of the m th ($m > 0$)-order anti-Stokes signal E_{ASm} can be expressed as

$$E_{ASm}(t) \propto \exp\{i[(m+1)\omega_{10} - m\omega_{20}]t + ((m+1)\phi_1(t) - m\phi_2(t))\},$$

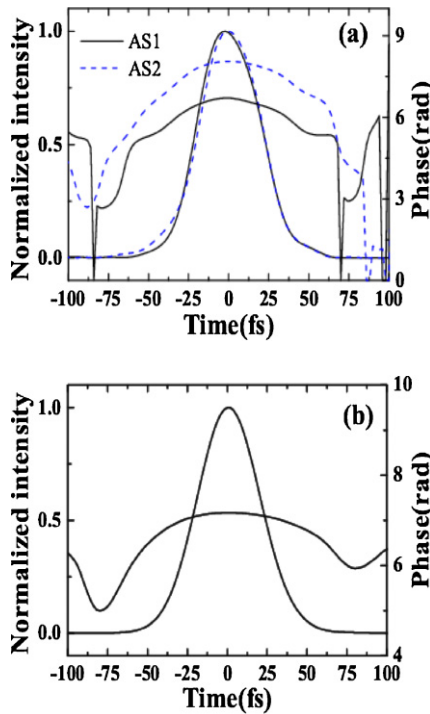


Fig. 4. (Color online) (a) Recovered intensity profiles and phases of AS1 (solid line) and AS2 (dashed line) with retrieval errors of 0.0119 and 0.0097. (b) Recovered pulse profile and phase of S1 with a retrieval error of 0.0049.

where ω_{10} , ω_{20} , ϕ_1 , ϕ_2 are the angle frequencies and phases of the two input beams, beam 1 and beam 2, respectively.

Given $\partial^2\phi_1(t)/\partial t^2 < 0$ (negative chirp) and $\partial^2\phi_2(t)/\partial t^2 > 0$ (positive chirp), we can obtain

$$\frac{\partial^2\phi_{ASm}(t)}{\partial t^2} = \frac{(m+1)\partial^2\phi_1(t)}{\partial t^2} - \frac{m\partial^2\phi_2(t)}{\partial t^2} < 0.$$

This indicates that the m th-order anti-Stokes signal is also negatively chirped. Nearly transform-limited pulses will be achieved when the negative chirp of the anti-Stokes sidebands just compensates the dispersion of the transparent bulk media and the phase change in the medium.

5. Conclusions

Frequency up-shifted and down-shifted microjoule multi-color femtosecond pulses were obtained at the same time by a cascaded FWM process in a fused silica glass plate. An approximately 45 fs laser pulse was obtained at around 950 nm. Self-compressed multicolor 20 fs pulses, which were nearly transform limited, were obtained when one of

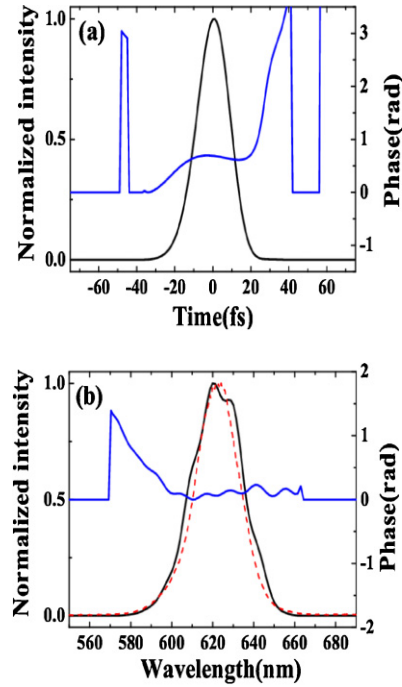


Fig. 5. (Color online) (a) Recovered intensity profile and temporal phase; (b) Recovered spectrum (black solid curve), spectral phase (blue solid curve), and measured spectrum (red dotted curve) of AS1.

the two input beams was negatively chirped and the other was positively chirped. The energy conversion efficiency from the sum of input beam energies to that of the sidebands was about 10%. The output sidebands can be used in various experiments, for example in a multicolor pump-probe experiment. In principle, there is no limitation to the output power as long as the input power is sufficiently high.

References

- 1) T. Kobayashi, A. Shirakawa, and T. Fuji: IEEE J. Sel. Top. Quantum Electron. **7** (2001) 525.
- 2) H. Crespo, J. T. Mendonça, and A. Dos Santos: Opt. Lett. **25** (2000) 829.
- 3) J. Liu and T. Kobayashi: Opt. Lett. **34** (2009) 1066.
- 4) J. Liu and T. Kobayashi: Opt. Express **17** (2009) 4984.
- 5) J. Liu and T. Kobayashi: Opt. Commun. **283** (2010) 1114.
- 6) J. Liu and T. Kobayashi: Opt. Express **16** (2008) 22119.
- 7) D. Pestov, R. K. Murawski, G. O. Ariunbold, X. Wang, M. C. Zhi, and A. V. Sokolov: Science **316** (2007) 265.
- 8) R. M. Hochstrasser: Proc. Natl. Acad. Sci. U.S.A. **104** (2007) 14190.